Experimental Study of the Role of Gas-Liquid Scheme Injector as an Acoustic Resonator in a Combustion Chamber

Haksoon Kim, Chae Hoon Sohn*
Department of Aerospace Engineering, Chosun University, Gwangju 501-759, Korea

In a liquid rocket engine, the role of gas-liquid scheme injector as an acoustic resonator or absorber is studied experimentally for combustion stability by adopting linear acoustic test. The acoustic-pressure signals or responses from the chamber are monitored by acoustic amplitude. Acoustic behavior in a rocket combustor with a single injector is investigated and the acoustic-damping effect of the injector is evaluated for cold condition by the quantitative parameter of damping factor as a function of injector length. From the experimental data, it is found that the injector can play a significant role in acoustic damping when it is tuned finely. The optimum tuning-length of the injector to maximize the damping capacity is near half of a full wavelength of the first longitudinal overtone mode traveling in the injector with the acoustic frequency intended for damping in the chamber. When the injector has large diameter, the phenomenon of the mode split is observed near the optimum injector length and thereby, the acoustic-damping effect of the tuned injectors can be degraded.

Key Words : Combustion Stability, Rocket Combustor, Injector, Acoustic Test, Acoustic Damping

1. Introduction

Acoustic instability or high-frequency combustion instability is a phenomenon that pressure oscillations are amplified through in-phase thermal interaction with combustion (Harrje and Reardon, 1972). This may result in an intense pressure fluctuation as well as excessive heat transfer to combustor walls in systems such as solid and liquid propellant rocket engines, ramjets, turbojet thrust augmentors, utility boilers, and furnaces (McManus et al., 1993). Accordingly, it has long gained significant interest in propulsion and power systems. Although it has caused common problems in these systems, it has been reported that it occurs most severely in liquid rocket engines due to their high energy density. Thermal damage on injector faceplate and combustor wall, severe mechanical vibration of rocket body, and unpredictable malfunction of engines, etc. are usual problems caused by acoustic instability. To understand this phenomenon, there have been conducted lots of studies (Harrje and Reardon, 1972; Culick and Yang, 1995; Oefelein and Yang, 1993; Ducruix et al., 2003), but it is still being pursued.

There have been adopted two methods in the control of acoustic instability, classified into passive and active controls (Culick and Yang, 1995; Laudien et al., 1995). Passive control is to attenuate acoustic oscillation using combustion stabilization devices such as baffles, acoustic resonators, and acoustic liners. For example, acoustic resonator can damp out or absorb pressure wave oscillating in the chamber using well-tuned cavity (Keller, 1974; Laudien et al., 1995). Although active control is studied and tested recently as an improved control method (Conrad et al., 2004),

* Corresponding Author,
E-mail : chsohn@chosun.ac.kr
TEL : +82-62-230-7123; **FAX** : +82-62-230-7123
Department of Aerospace Engineering, Chosun University, Gwangju 501-759, Korea. (Manuscript **Received** November 10, 2005; **Revised** March 29, 2006)

the most reliable method to suppress acoustic-pressure oscillation is still to install baffle or resonators on/near the injector faceplate. However, the devices are installed additionally and inevitably to suppress undesirable acoustic oscillations if they should be. And thus, negative effects of engine-performance degradation and complexity in engine manufacture can be caused by the installation of these devices.

On the other hand, in liquid rocket engines, injectors are mounted necessarily to the faceplate in order to inject propellants into the chamber. Depending on the phase of the injected propellants, they are classified into liquid-liquid scheme and gas-liquid scheme injectors. In the pump-fed liquid rocket engines, staged combustion cycle is usually employed for high performance and efficiency, where preburner is used and regenerative cooling is adopted for the cooling of combustor wall (Huzel and Huang, 1992). In this system, a coaxial and gas-liquid scheme injector is typically used, which is illustrated in Fig. 1(a). As one example of injection pattern, the figure shows that gaseous oxygen (GO_2) flows through the inner passage of the injector and then, it is mixed with liquid hydrocarbon fuel injected through several peripheral holes and finally, both GO_2 and liquid fuel are injected into the chamber (Sutton, 2001). At this point, with the inside volume of the injector occupied by gas, it is worthy of note that the gas-liquid scheme injectors may play a significant role in acoustic damping like acoustic resonators in addition to its original function of propellants injection. If it is true of the injector, proper design of the injector will attenuate pressure oscillation to a good degree and eventually, we can do without additional installation of baffle or resonator.

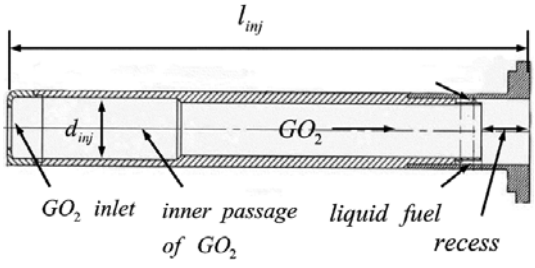

(a) Coaxial gas-liquid scheme injector

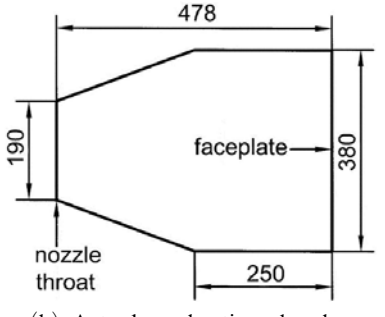

(b) Actual combustion chamber

Fig. 1 Schematic diagrams of the coaxial gas-liquid scheme injector and the actual combustion chamber (unit : mm)

In this regard, the role of gas-liquid scheme injector as acoustic resonator or absorber is investigated here. The present study provides new information on injector design for acoustic stability ; the possibility of acoustic damping by tuning the injector and the optimum size or length of the injector for maximum acoustic damping. For this, acoustic behaviors in the chamber with a single injector are investigated experimentally by adopting linear acoustic test. Out of several acoustic modes, acoustic damping of the 1st tangential mode is emphasized because it is known to be one of the most destructive modes in a rocket combustor (Harrje and Reardon, 1972).

2. Experimental Methods

2.1 Combustion chamber and injector

The geometries of the injector and the sample chamber to be analyzed are shown in Fig. 1. Usually, the combustion chamber of a liquid rocket engine has numerous injectors mounted to the faceplate. But, all of the injectors do not need to be considered in order to investigate effects of the injector on acoustic damping. Accordingly, the chamber with a single injector is considered. The chamber domain ranges from the injector faceplate to nozzle throat including injector itself. The sample chamber has the typical geometry of liquid rocket combustion chamber. The diameters of the chamber and the nozzle throat, D_{ch} and D_{th}, are 380 and 190 mm, respectively. The lengths from the faceplate to nozzle entrance and

the throat, L_e and L_{th}, are 250 and 478 mm, respectively and a half contraction angle in the conical section is 30°. Although the inner passage of the gas-liquid scheme injector can frequently have tapered or stepped shapes as shown in Fig. 1(a), the straight passage is assumed here for simplicity and clarity of acoustic investigation. Besides, it is assumed that the injector has no recess for the same purpose. Accordingly, it has completely cylindrical shape. Three injector diameters, d_{inj} of 7, 14, and 20 mm are selected and the baseline diameter is 7 mm. On the other hand, the injector length, l_{inj} is adjusted for acoustic tuning in this study and thus, acoustic field is calculated with a variable parameter of l_{inj}.

In this test, the chamber wall and the faceplate have the rigid wall made of acrylic material. In actual reactive flows, the sonic condition is formed at the nozzle throat and thus, the throat can be considered to be acoustically closed end which reflects all the incident waves without acoustic loss or amplification. In other words, it acts as a rigid wall on acoustics although it has physically open condition for mean flow. For this reason, the chamber shown in Fig. 1(b) has the rigid wall at the nozzle throat and excludes the nozzle expansion part downstream of the throat since the part does not affect the acoustic field within the chamber. Injector is also made of acrylic material.

It has been reported that acoustic tests or calculations for cold condition can offer good results and information in the acoustic point of view although combustion processes are not considered (Harrje and Reardon, 1972 ; Laudien et al., 1995 ; Keller, 1974). Wet acoustic tests, where spray distribution is considered, can produce more realistic acoustics near the injector faceplate than dry tests. Nevertheless, the fundamentals are maintained in dry tests. Accordingly, dry acoustic tests are conducted here for cold-volume condition without mean flow. That is, the medium is assumed to be a quiescent air of which density, ρ_{ch} and sound speed, c_{ch} are 1.2 kg/m^3 and 343 m/s at 20℃, respectively.

2.2 Acoustic-test apparatus and test procedures

Schematic diagram of the acoustic-test apparatus is shown in Fig. 2. The combustion chamber is installed in the horizontal position and operates at atmospheric pressure. For acoustic excitation, ransom-noise signal is generated by notebook computer, sent to amplifier (Inter M model QD-4960), where the signal is amplified, and finally sent to the loudspeaker. It is also sent to FFT (Fast Fourier Transform) spectrum analyzer through input-signal channel (Ch1). The loudspeaker is located on the faceplate near the chamber wall and imposes acoustic excitation into the chamber. The present test is linear acoustic test, i.e., the amplitude of acoustic pressure excited in the chamber is small and within a linear range. The acoustic-pressure signals or responses from

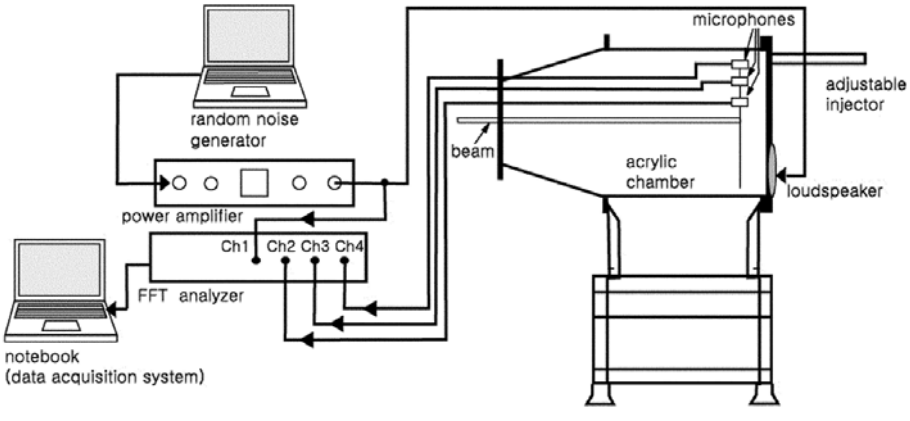

Fig. 2 Schematic diagram of acoustic-test apparatus

the chamber are monitored by acoustic amplitude, which is measured by the microphone. Three microphones are mounted by the horizontal beam and installed radially as shown in Fig. 2. The mounting beam can rotate to measure the spatial distribution of the acoustic amplitude. Their locations correspond to the monitoring points. The most principal point is located on the outermost point near the chamber wall at the opposite side to the loudspeaker, where the clearest signal can be measured with respect to the 1st tangential mode (Sohn, 2002; Sohn et al., 2004). The signals measured by the microphones are sent to the spectrum analyzer, through which FRF (Frequency Response Function) is obtained. From FRF data, the acoustic resonance, the resonant frequencies, and the acoustic modes are identified. The details on the acoustic test can be also found elsewhere (Laudien et al., 1995; Ko et al., 2004).

It can be found that the resonant frequencies of the adopted chamber have $O(100\,\text{Hz})$ at the lower acoustic modes from the analytic calculations (Zucrow, 1977). For example, the resonant frequencies of the two principal transverse oscillatory modes, 1T (the 1st tangential mode) and 1T1L (the combined acoustic mode of the 1st tangential and the 1st longitudinal modes) are estimated to be $f_{1T}=548$ Hz and $f_{1T1L}=766$ Hz, respectively. Accordingly, we have verified that the random-noise signal has the constant acoustic intensity irrespective of frequency over the frequency range of 200~800 Hz. First, the acoustic -pressure signals are measured in the chamber without the injector and then, they are measured in the chamber with a injector as a function of the length of the injectors with several diameters.

2.3 Consideration of injector's role as an acoustic resonator

Acoustic resonators or absorbers have several shapes for the sake of combustion stabilization. One of them, quarter-wave resonator is illustrated in Fig. 3(a). The simplified gas-liquid scheme injector has the same shape as quarter-wave resonator, but with different boundary condition at one end surface. That is, quarter-wave resonator has an open end at the matching surface with the chamber and a closed end at the other as shown in Fig. 3(a), whereas the present injector has open ends at both ends as shown in Fig. 3(b).

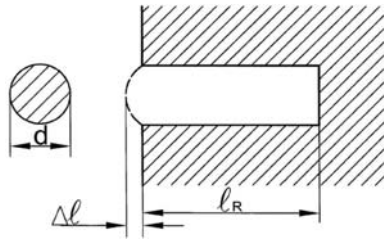

(a) Quarter-wave resonator

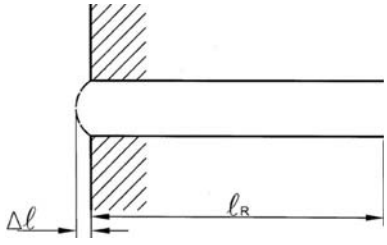

(b) Half-wave resonator

Fig. 3 Quarter-wave and half-wave resonators

In accordance with these boundary conditions at end surfaces, acoustic-pressure node and antinode (Kinsler et al., 2000) are formed at one end and the other, respectively, in quarter-wave resonator. Therefore, it functions literally as quarter-wave resonator. In a similar manner, the present injector may function as half-wave resonator since acoustic pressure nodes are formed at both ends of the injector. It is predicted that wave cancellation, the mechanism of acoustic damping occurring in quarter-wave resonator (Harrje and Reardon, 1972; Laudien et al., 1995; Keller, 1974) can be applied to the injector as well. The only difference between them is the wavelength; a quarter and a half of a full wavelength, respectively.

The tuning frequency of quarter-wave resonator is expressed by (Laudien et al., 1995)

$$f_0=\frac{c_R}{4(l_R+\Delta l)} \tag{1}$$

where f_0 denotes tuning frequency, i.e., the frequency of harmful acoustic oscillation intended to be damped in the chamber, c_R sound speed of the fluid inside the resonator, l_R the length of the resonator, and Δl length or mass correction fac-

tor. The correction factor can be calculated approximately for various conditions (Keller, 1974). If the hypothesis aforementioned is valid, Eq. (1) can be still used even for injector design with the substitution of a numeral "2" for "4" of Eq. (1). And then, the optimum length of the injector for maximum acoustic damping is derived as

$$l_{inj}=\frac{c_{inj}}{2f_0}-\Delta l \tag{2}$$

where l_{inj} and c_{inj} denote the injector length and sound speed of the fluid inside the injector, respectively. This equation expresses theoretically the optimum length of the injector canceling the acoustic oscillation coming from the chamber with the frequency of f_0. Out of numerous acoustic modes, the first tangential (1T) mode is intended to be damped by the injector in this study. But, the present results can be applied to any acoustic modes.

3. Results and Discussions

3.1 Acoustic-pressure response and damping

First, in the chamber without the injector, the acoustic-pressure signal measured at the monitoring point is processed by FFT analyzer and the resultant amplitude spectrum is shown in Fig. 4. From the spatial distribution of the acoustic amplitude, the resonant acoustic mode at each peak is identified as follows ; the 1st longitudinal (1L), the 1st tangential (1T), the 2nd longitudinal (2L) modes, and so on. The 1T mode resonant at f_{1T}=558 Hz has the largest amplitude. It is intended to be damped by the injector tuning in the present study.

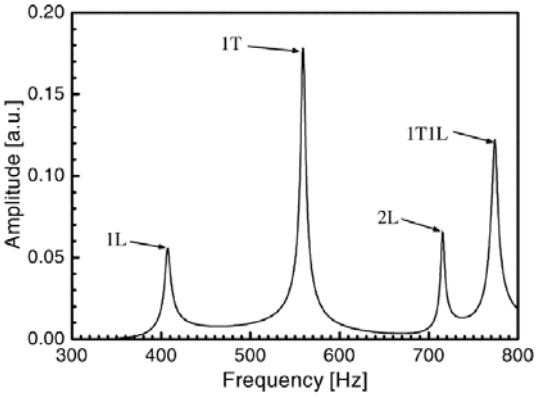

Fig. 4 Acoustic-pressure responses in the chamber without the injector

Next, a single injector of d_{inj}=7 mm is installed at the faceplate. The acoustic-pressure responses are obtained in the chamber with the injectors of l_{inj}=150 and 302 mm and are shown in Fig. 5 compared with the original response in the chamber without the injector (i.e., l_{inj}=0 mm). As shown in the figure, the acoustic amplitude of 1T mode is affected appreciably by the change of injector length. With l_{inj}=302 mm, the peak amplitude is much lower than the original amplitude. Acoustic-pressure responses in Fig. 5 indicate that the injector can play a significant role in acoustic damping. To evaluate acoustic damping capacity of the injector quantitatively, a parameter of damping factor, is introduced and evaluated by bandwidth method in the form (Laudien et al., 1995 ; Kim et al., 2004),

$$\eta=\frac{f_2-f_1}{f_{peak}} \tag{3}$$

where f_{peak} is the frequency at which the peak response (p_{peak}) appears and f_1 and f_2 are the frequencies at which the pressure amplitude corresponds to $p_{peak}/\sqrt{2}$ with $f_2>f_1$. This equation indicates that the damping factor becomes higher as the bandwidth normalized by the peak fre-

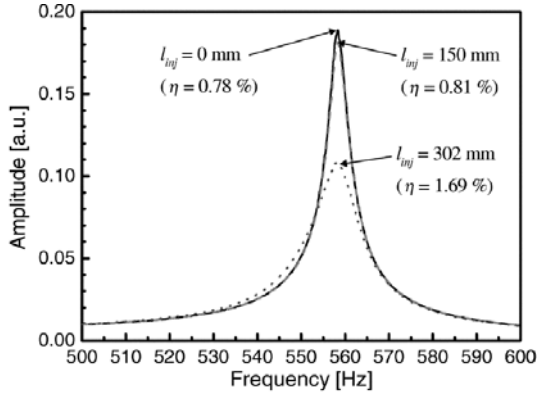

Fig. 5 Acoustic-pressure responses near f_{1T} for several lengths of l_{inj}=0, 150, and 302 mm in the chamber with a single injector of d_{inj}= 7 mm

quency, f_{peak}, is broadened on the plot of the excitation frequency versus acoustic-pressure amplitude. That is, higher damping factor indicates weaker resonance. Since acoustic instability results from strong or sharp acoustic resonance, the damping factor is used as its quantitative parameter instead of the acoustic amplitude.

Based on the acoustic-response data measured with variable injector length, acoustic amplitudes and frequencies at 1T mode are shown as a function of l_{inj} in Fig. 6 and damping factors calculated by Eq. (3) are shown in Fig. 7. As l_{inj} increases from 0, acoustic amplitude maintains constant value and decreases abruptly near $l_{inj}=$ 300 mm. This pattern is repeated with further increase in the injector length. As shown in Fig. 7, damping factor increases gradually and then, does rapidly near $l_{inj}=300$ mm. As l_{inj} increases further, damping factor decreases rapidly and then, the similar cyclic pattern is repeated. Two peaks of η occur near $l_{inj}=300$ and 600 mm. With $f_{1T}=558$ Hz, the wavelength of the first longitudinal overtone mode inside the injector is calculated to be 615 mm for cold condition of $c_{inj}=343$ m/s. Accordingly, the injector length of 302 mm, at which the largest peak occurs, corresponds to a half wavelength of 1L-mode oscillating in the injector with the same frequency as the frequency of 1T mode in the chamber. The exact length of a half wavelength, $(1/2)\lambda$ is calculated to be 307.5 mm and the error of 5.5 mm can be attributed to the length correction, Δl as indicated in Eq. (2).

From Fig. 7, the second largest peak occurs at $l_{inj}=610$ mm, which corresponds to λ. Although not shown here, the subsequent peaks have been observed in order at $l_{inj}=(3/2)\lambda$, 2λ, and $(5/2)\lambda$, etc. All of these lengths satisfy open condition at both ends of the injector and thus, integer multiples of $(1/2)\lambda$ correspond to tuning length of the injector for efficient acoustic damping. Out of them, the optimum tuning length is a half wavelength at which maximum damping capacity is made as shown in Fig. 7. This point also verifies that wave cancellation is the key mechanism of acoustic damping caused by the present injector although there is acoustic absorption at the wall boundary inside the injector.

3.2 Verification of acoustic test with open-end inlet condition

In the preceding section, it has been found that the injector with an open inlet can work as a half-wave resonator for acoustic damping. But, compared with the closed-end condition, it is difficult to realize perfectly the open condition at the injector inlet because the experimental apparatus including the injector is installed in the confined room. This can cause wave reflection at the wall of the room and the reflected wave may enter the injector through its inlet. This may interferes the complete open condition. To verify the completeness of the open-inlet condition, the test is repeated with the injector which has the closed-end inlet and 1.5 times longer length than the

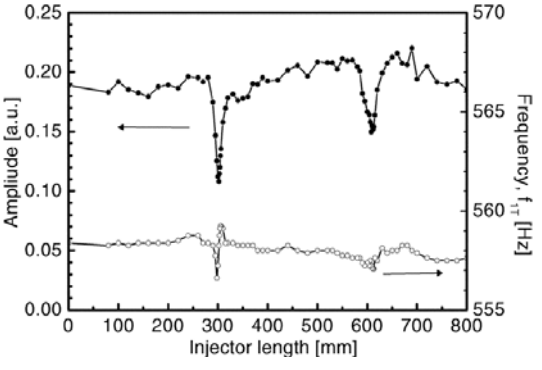

Fig. 6 Acoustic amplitudes and frequencies as a function of injector length at 1T mode ($d_{inj}=$ 7 mm)

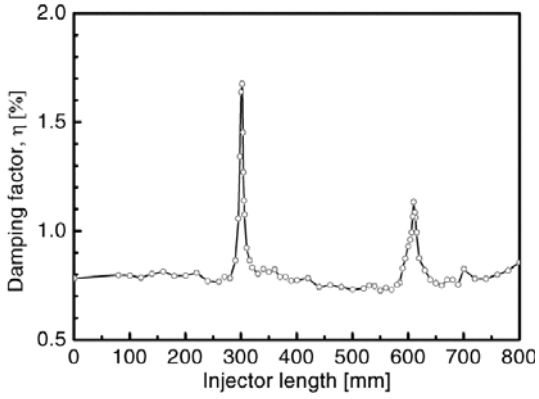

Fig. 7 Damping factors as a function of injector length at 1T mode ($d_{inj}=7$ mm)

original injector. The longitudinal acoustic oscillations within both original and elongated injectors are schematically shown in Fig. 8. The elongated injector with closed-inlet condition has the same acoustic-oscillation pattern as the original injector with open-inlet condition. Accordingly, the test with the former injector will produce the equivalent data theoretically.

The test data are compared with the original data in Fig. 9. Two data are comparable to each other and shown nearly identical pattern. With respect to finding the optimum length of the injector, the lengths of 302 mm and 303.3 mm can be proposed in both tests, respectively. The error between two values is negligible. The length of 303.3 mm is equivalent to the optimum injector length of 455 mm with the closed-inlet condition ; 303.3 mm=455/1.5. Although the quantification of the completeness of the open-inlet condition is more complex, the present test can produce reliable data for injector tuning with negligible error.

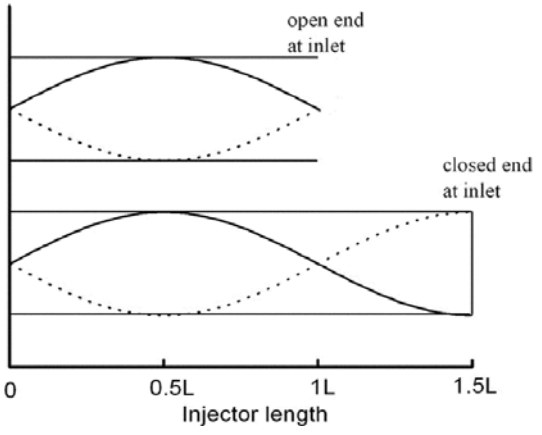

Fig. 8 Longitudinal acoustic oscillations within the injector with open end and the elongated injector with closed end at injector inlet

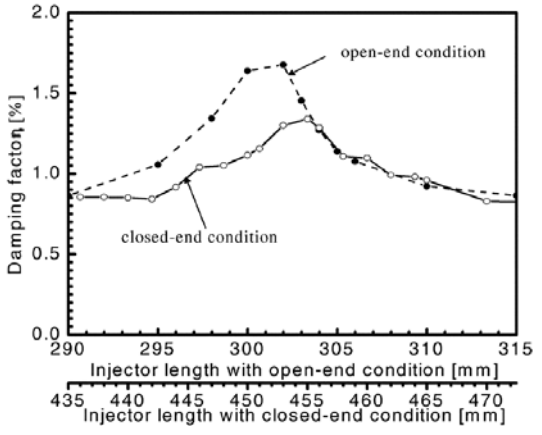

Fig. 9 Damping factors for open-end and closed-end conditions (d_{inj}=7 mm)

3.3 Effect of the injector diameter

The injectors with the other diameters, d_{inj}=14 and 20 mm, are tested. With three diameters of d_{inj}=7, 14, and 20 mm, the ratio of the opening areas of the injectors is about 1 : 4 : 8. The acoustic-pressure responses are measured in the chamber with the variable-length injectors of d_{inj}=14 mm and are shown in Fig. 10. It is worthy of note that at l_{inj}=290 mm, one peak is splitted into two peaks, i.e., lower and upper peaks, of which amplitudes are much lower than the original amplitude. This phenomenon is called mode split (Harrje and Reardon, 1972 ; Natanzon, 1986). The mode split is observed as well in case of the injectors with d_{inj}=20 mm and $l_{inj}\approx$300 mm. With d_{inj}=14 and 20 mm, the mode split is observed over the ranges of l_{inj}=290~315 mm and 285~340 mm, respectively. While mode split is observed for the shortest injector length of 285 mm and in the widest range of l_{inj} in case of d_{inj}= 20 mm, the phenomenon is not observed with the injector of the smallest diameter of 7 mm.

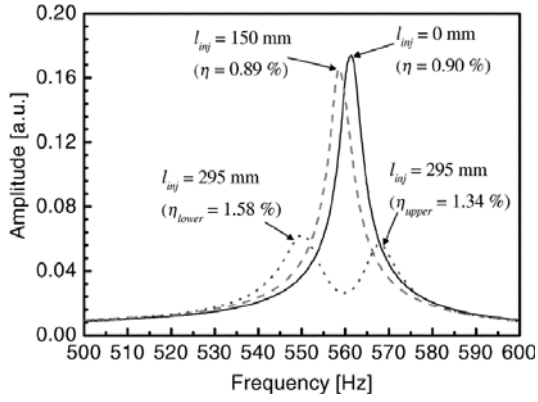

Fig. 10 Acoustic-pressure responses near f_{1T} for several lengths of l_{inj}=0, 150, and 290 mm in the chamber with a single injector of d_{inj}= 14 mm

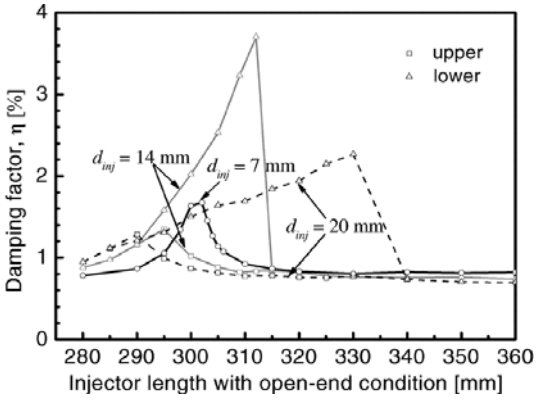

Fig. 11 Damping factors for several diameters of d_{inj}=7, 14, and 20 mm in the chamber with a single injector

Acoustic-pressure responses in the chamber with three injectors of d_{inj}=7, 14, and 20 mm are measured as a function of l_{inj} near $(1/2)\lambda$ and the calculated damping factors are shown in Fig. 11. Damping factor is relatively higher at l_{inj} close to $(1/2)\lambda$. Accordingly, it is found that all the injectors maintain the acoustic behavior of a half-wave resonator irrespective of the diameter.

At shorter length than the critical value, at which mode split starts, damping factor increases gradually with the injector diameter as shown in Fig. 11. But, this favorable effect of the diameter on acoustic damping is degraded by mode split. That is, damping factors at lower and upper peaks of the splitted mode are not increased with the diameter at $l_{inj}=(1/2)\lambda$. On the other hand, it is a favorable effect that large damping factors are maintained over the wider range of l_{inj} as the diameter increases.

4. Concluding Remarks

Acoustic-pressure responses in the chamber with gas-liquid scheme injector have been investigated experimentally by adopting linear acoustic test. This experimental study is intended to check the possibility of stability enhancement through injector tuning and the role of the injector as acoustic resonator or absorber is studied in the chamber with a single injector. The first tangential mode has been selected a target mode to be damped or absorbed in this study.

Acoustic behaviors in the chamber with a single injector have shown that the injector can absorb acoustic oscillation in the chamber most effectively when it has the tuning length of a half wavelength with respect to the acoustic frequency to be damped. In other words, it acts effectively as a half-wave resonator; the optimum length for acoustic tuning is about a half wavelength. Since mode split is observed in the injector with large diameters, the optimum length has the range near the length of a half wavelength. From the acoustic tests, it has been found that effects of the injector on acoustic damping are critical and significant. Accordingly, it is proposed that the damping effect should be considered elaborately in injector design. As the injector diameter increases, the acoustic damping capacity is enhanced further unless the mode split shows up.

Although the first tangential mode is concentrated on in this study, the present findings are not limited to the specific acoustic mode, but applicable to any acoustic modes. Based on the present data, it is proposed that the injector should be designed for propellants injection and at the same time, for acoustic damping since acoustic stability can be improved considerably when it is tuned finely or properly.

Acknowledgments

This study was supported in part by research funds from Chosun University, 2005.

References

Culick, F. E. C. and Yang, V., 1995, in *Liquid Rocket Engine Combustion Instability* (Edited by Yang, V. and Anderson, W. E.), *Progress in Astronautics and Aeronautics*, Vol. 169, AIAA, Washington DC, pp. 3~37.

Conrad, T., Bibik, A., Shcherbik, D., Lubarsky, E. and Zinn, B. T., 2004, "Control of Instabilities in Liquid Fueled Combustor by Modification of the Reaction Zone Using Smart Fuel Injector," AIAA Paper 2004-4029.

Ducruix, S., Schuller, T., Durox, D. and Candel,

S., 2003, "Combustion Dynamics and Instabilities: Elementary Coupling and Driving Mechanisms," *Journal of Propulsion and Power*, Vol. 19, No. 5, pp. 722~734.

Harrje, D. J. and Reardon, F. H. (eds.), 1972, *Liquid Propellant Rocket Combustion Instability*, NASA SP-194.

Huzel, D. K. and Huang D. H., 1992, *Modern Engineering for Design of Liquid-Propellant Rocket*, Vol. 147, Progress in Astronautics and Aeronautics, AIAA, Washington, DC, p. 35.

Keller, Jr., R. B. (ed.), 1974, *Liquid Rocket Engine Combustion Stabilization Devices*, SP-8113, NASA.

Kim, S.-K., Kim, H. J., Seol, W. S. and Sohn, C. H., 2004, "Acoustic Stability Analysis of Liquid Propellant Rocket Combustion Chambers," AIAA Paper 2004-4142.

Kinsler, L. E., Frey, A. R., Coppens, A. B. and Sanders, J. V., 2000, Fundamentals of Acoustics, 4th Ed., John Wiley & Sons, Inc., NY, Chap. 2.

Ko, Y. S., Lee, K. J. and Kim, H. J., 2004, "Acoustic Tests on Atmospheric Condition in a Liquid Rocket Engine Chamber," *Transactions of the KSME (B)* (in Korea), Vol. 28, No. 1, pp. 16~23.

Laudien, E., Pongratz, R., Pierro, R., and Preclik, D., 1995, in *Liquid Rocket Engine Combustion Instability* (Edited by Yang, V. and Anderson, W. E.), *Progress in Astronautics and Aeronautics*, Vol. 169, AIAA, Washington DC, pp. 377~399.

McManus, K. R., Poinsot, T. and Candel, S. M., 1993, "A Review of Active Control of Combustion Instabilities," *Progress in Energy and Combustion Science*, Vol. 19, pp. 1~29.

Natanzon, M. S., 1986, *Combustion Instability* (Translated by Culick, F. E. C. in 1966), Mashinostroyeniye, Moscow.

Oefelein, J. C. and Yang, V., 1993, "Comprehensive Review of Liquid-Propellant Combustion Instabilities in F-1 Engines," *Journal of Propulsion and Power*, Vol. 9, No. 5, pp. 657~677.

Sohn, C. H., 2002, "A Numerical Study on Acoustic Behavior in Baffled Combustion Chambers," *Transactions of the KSME (B)* (in Korea), Vol. 26, No. 7, pp. 966~975.

Sohn, C. H., Kim. S.-K. and Kim, Y.-M., 2004, "Effects of Various Baffle Design on Acoustic Characteristics in Combustion Chamber of Liquid Rocket Engines," *KSME International Journal*, Vol. 18, No. 1, pp. 154~161.

Sutton, G. P., 2001, *Rocket Propulsion Elements*, 7th Ed., John Wiley & Sons, Inc., New York.

Zucrow, M. J. and Hoffman, J. D, 1977, *Gas Dynamics*, Vol. II, John Wiley & Sons, Inc., New York.